*Research Article*

# Efficient Synthesis of Single-Chain Polymer Nanoparticles *via* Amide Formation

## Ana Sanchez-Sanchez[1,2] and José A. Pomposo[1,2,3]

[1]*Centro de Física de Materiales (CSIC, UPV/EHU), Paseo Manuel de Lardizabal 5, 20018 San Sebastián, Spain*
[2]*Departamento de Física de Materiales, Universidad del País Vasco (UPV/EHU), Paseo Manuel de Lardizabal 3, 20018 San Sebastián, Spain*
[3]*IKERBASQUE, Basque Foundation for Science, María Díaz de Haro 3, 48013 Bilbao, Spain*

Correspondence should be addressed to José A. Pomposo; josetxo.pomposo@ehu.es

Single-chain technology (SCT) allows the transformation of individual polymer chains to folded/collapsed unimolecular soft nanoparticles. In this work we contribute to the enlargement of the SCT toolbox by demonstrating the efficient synthesis of single-chain polymer nanoparticles (SCNPs) *via* intrachain amide formation. In particular, we exploit cross-linking between active methylene groups and isocyanate moieties as powerful "click" chemistry driving force for SCNP construction. By employing poly(methyl methacrylate)- (PMMA-) based copolymers bearing $\beta$-ketoester units distributed randomly along the copolymer chains and bifunctional isocyanate cross-linkers, SCNPs were successfully synthesized at r.t. under appropriate reaction conditions. Characterization of the resulting SCNPs was carried out by means of a combination of techniques including size exclusion chromatography (SEC), infrared (IR) spectroscopy, proton nuclear magnetic resonance ($^1$H NMR) spectroscopy, dynamic light scattering (DLS), and elemental analysis (EA).

## 1. Introduction

Single-chain technology (SCT) is a new paradigm for the future construction of smart and autonomous soft nanodevices [1]. Nowadays, SCT allows the transformation of individual polymer chains to folded/collapsed unimolecular soft nanoparticles, the so-called single-chain polymer nanoparticles (SCNPs) [2–5]. The compaction of synthetic polymers to SCNPs has some resemblance to the folding of proteins to their native state, although it is still far from the perfection found in natural macromolecules [6]. Significant effort has been spent in recent years to endow SCNPs with bioinspired functions trying to mimic those found in natural polypeptides (both folded proteins and intrinsically disordered proteins) such as enzymatic activity and selectivity [7–9], or multibinding activity and transport properties [10, 11]. Currently, SCNPs are synthesized through one of the following techniques: (i) intrachain homocoupling, (ii) intrachain heterocoupling, or (iii) cross-linker mediated collapse [4]. Concerning the nature of the intrachain cross-linking reaction, it can be irreversible (covalent bonds) or reversible (noncovalent or dynamic covalent bonds) [3]. Irreversible SCNPs have been synthesized by means of different intrachain cross-linking reactions [12–36].

First reports about the synthesis of permanent SCNPs by means of the intrachain homocoupling technique under high dilution conditions by Mecerreyes et al. relied on the use of poly(styren)-, poly(alkyl methacrylate)-, and poly($\varepsilon$-caprolactone)-based precursors containing vinyl reactive functional groups [12]. Unsaturated functional groups were also used for synthesizing poly(4-N-Boc-aminostyrene)- and poly(carbonate)-based SCNPs by Jiang and Thayumanavan and Cherian et al., respectively [13, 14]. Poly(styrene)- and poly(alkyl methacrylate)-based unimolecular nanoparticles were synthesized in multigram quantities by Harth and coworkers using benzocyclobutene containing precursors *via* intramolecular Diels-Alder reactions at very high temperature (250°C) [15]. Later, benzosulfone-decorated

poly(styrene)- and poly(cyclohexyl acrylate)-based precursors were synthesized by Harth and coworkers for the preparation of individual unimolecular nanoparticles *via* quinodimethane formation, although cross-linking reaction conditions were still very harsh (250°C) [16, 17]. Poly(methyl methacrylate)-based SCNPs have been obtained by Zhu et al. *via* intramolecular Bergman cyclization at relatively lower temperatures (150°C) [18, 19]. The synthesis of poly(styrene)- and poly(alkyl methacrylate)-based unimolecular nanoparticles *via* intramolecular cross-linking of sulfonyl azide- [20] and benzoxazine- [21] functionalized polymers still required very high temperatures (190–200°C). To solve the potential problems of precursor and nanoparticle thermal degradation, a new route was introduced by Sanchez-Sanchez et al. where naked propargylic-decorated single-chain nanoparticle precursors synthesized *via* redox-initiated reversible addition-fragmentation chain transfer (RAFT) polymerization were intrachain collapsed at room temperature under normal air conditions by means of Glaser-Hay coupling (C-C "click" chemistry) [22]. Recently, the $B(C_6F_5)_3$-promoted collapse of linear polymer precursors containing epoxide groups to SCNPs endowed with catalytic activity has been carried out by Perez-Baena et al. [23]. Using a similar approach, Wong et al. have developed biocompatible SCNPs which were found to be nontoxic toward human embryonic kidney cells [24]. Poly(styrene)-based unimolecular nanoparticles have been prepared by Dirlam et al. through intrachain cross-linking *via* oxidative polymerization of 3,4-propylenedioxy-thiophene functional groups at 50°C [25]. More recently, a facile strategy for preparation of SCNPs by intramolecular photo-cross-linking of azide polymers has been reported by Li et al. [26], and fluorescence-labeled hydrophilic SCNPs have been synthesized by Wang et al. *via* single-chain folding of precursors containing fluorescent anthracene and crosslinkable oxazine groups [27].

The fabrication of SCNPs has been also carried out using the intrachain heterocoupling technique. A representative example of the use of the intrachain heterocoupling technique was the construction of permanent SCNPs through highly efficient azide-alkyne "click" chemistry (i.e., copper-catalyzed [3 + 2] cycloaddition of alkynes and azides, CuAAC) [28]. By employing this technique, biofunctionalized poly(methyl methacrylate)-based unimolecular nanoparticles were prepared at room temperature in high yield based on azide- and protected alkyne-decorated polymer precursors by Ruiz de Luzuriaga et al. [28]. The technique was further simplified by Oria et al. starting with copolymers containing protected alkyne groups as well as chloromethyl groups that were transformed rapidly and quantitatively to azidomethyl groups by means of a simple substitution reaction using sodium azide [29]. The intrachain heterocoupling technique has been also used to prepare thermoresponsive SCNPs by Ormategui et al. [30]. More recently, photo-induced Diels-Alder ligation and nitrile imine mediated tetrazole-ene cycloaddition have been used by Barner-Kowollik and colleagues to synthesize well-defined functional and fluorescent SCNPs, respectively [31, 32].

Bifunctional cross-linker mediated collapse of polymer chains is another efficient and straightforward method for
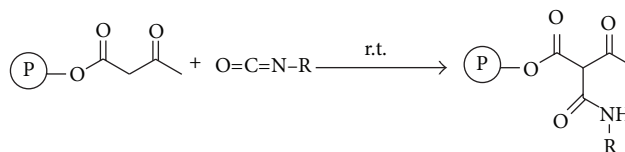


FIGURE 1: Schematic illustration of amide formation upon the "click" chemistry reaction at r.t. between a $\beta$-ketoester moiety and an isocyanate compound (P = polymer chain; R = alkyl substituent).

obtaining SCNPs. Water-soluble poly($\gamma$-glutamic acid)-based SCNPs were fabricated by Radu et al. through the cross-linker-induced collapse technique by using a biosynthetic poly($\gamma$-glutamic acid) precursor and 2,2′-(ethylenedioxy)diethylamine as bifunctional cross-linker in the presence of carbodiimide as catalyst [33]. The synthesis of poly(methyl methacrylate)- and poly(styrene)-based SCNPs by intramolecular cross-linking of isocyanate-functionalized copolymers with diamines *via* urethane formation was reported by Beck et al. [34]. Additionally, the high versatility of the cross-linker induced collapse method *via* intrachain CuAAC was demonstrated by Ruiz de Luzuriaga et al. in 2010 during the facile synthesis of SCNPs of very different chemical nature [35]. Michael addition reaction was employed by Sanchez-Sanchez et al. to synthesize poly(methyl methacrylate)-based SCNPs mimicking transient-binding disordered proteins under mild reaction conditions (at room temperature and in the presence of oxygen) [10]. More recently, unimolecular polymer nanoparticles have been formed by Hansell et al. by employing polystyrenes decorated with pendent norbornenes and a bifunctional tetrazine cross-linker, demonstrating that the formation of SCNPs can be carried out *via* tetrazine-norbornene coupling [36].

In this work, we contribute to the enlargement of the toolbox of single-chain technology by demonstrating the efficient synthesis of SCNPs *via* amide formation. In particular, we exploit, as powerful driving force for SCNP construction, the intrachain cross-linking through amide formation between active methylene groups and isocyanate moieties (see Figure 1). SCNP synthesis has been carried out by employing the technique of bifunctional cross-linker mediated collapse. The resulting SCNPs have been characterized by a combination of complementary techniques including SEC, IR spectroscopy, $^1$H NMR spectroscopy, DLS, and EA.

## 2. Materials and Methods

*2.1. Materials.* Methyl methacrylate (MMA) (99%), 2-acetoacetoxy ethyl methacrylate (AEMA) (95%), 2,2-azobis (2-methylpropionitrile) (AIBN) (≥98%), 1,5-diazabicyclo[4.3.0]non-5-ene (DBN) (98%), hexamethylene diisocyanate (HMDI) (≥99.0%), 1 M HCl, ethyl acetate (anhydrous, 99.8%), diethyl ether (ACS reagent, anhydrous, >99.0%), chloroform (≥99%), tetrahydrofuran (anhydrous, ≥99.9%), and deuterated chloroform (99.96 atom% D, containing 0.03% (v/v) tetramethylsilane, TMS) were purchased from
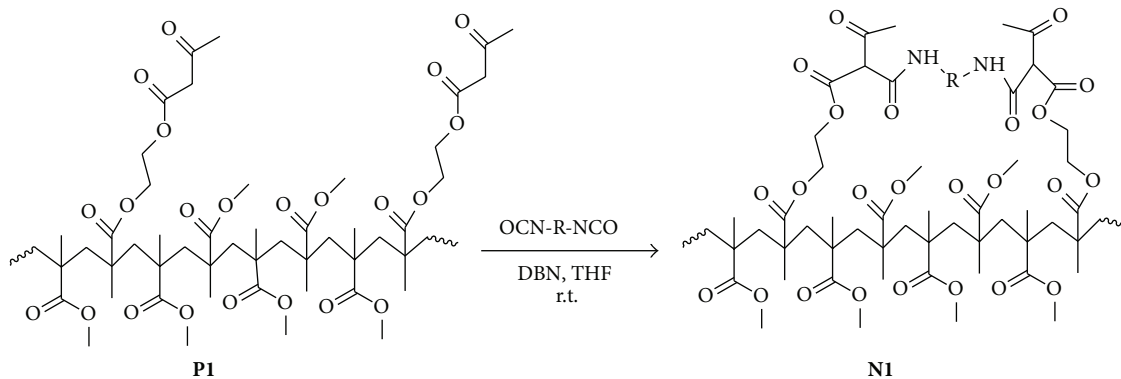
Figure 2: Synthesis route to SCNPs *via* intrachain amide formation at high dilution (OCN–R–CNO = bifunctional isocyanate compound; DBN = 1,5-diazabicyclo[4.3.0]non-5-ene; THF = tetrahydrofuran).

Aldrich and used, unless specified, as received. 2-Cyanoprop-2-yl-dithiobenzoate (CPDB) (≥97%) was purchased from Strem Chemicals. Methanol (synthesis grade) was purchased from Scharlab. MMA was purified by distillation before use. AEMA was purified by passing through basic alumina.

*2.2. Synthesis of SCNP Precursors.* MMA (1 mL, 9.4 mmol), AEMA (0.6 mL, 3.1 mmol), CPDB (**P1**: 9.0 mg, 0.33 mmol; **P2**: 2.76 mg, 0.1 mmol), and AIBN (**P1**: 1 mg, $6 \times 10^{-2}$ mmol; **P2**: 2 mg, $3 \times 10^{-2}$ mmol) were dissolved in ethyl acetate (3.2 mL). The reaction mixture was degassed by passing argon for 15 min. The copolymerization reaction was carried out at 65°C for 18 h. The resulting SCNP precursors (**P1** or **P2**; see Figure 2) were isolated by precipitation in methanol and further drying (**P1**: yield (%) = 46, $M_w$ (SEC/SLS) = 40.9 kDa, $M_w/M_n$ = 1.05, and composition ($^1$H NMR) = 30 mol% AEMA; **P2**: yield (%) = 70, $M_w$ (SEC/SLS) = 248.1 kDa, $M_w/M_n$ = 1.35, and composition ($^1$H NMR) = 27 mol% AEMA).

*2.3. Synthesis of SCNPs.* The SCNP precursor (**P1**: 100 mg, 0.32 mmol; **P2**: 100 mg, 0.31 mmol) and catalyst (DBN, 13.8 μL, 0.1 mmol) were first dissolved in dry THF (100 mL) at room temperature. After degassing the mixture by passing argon for 15 min the bifunctional isocyanate cross-linker was added by using a vacuum syringe (HMDI, 25.8 μL, 0.16 mmol). The progressive folding/collapse process was followed through SEC/SLS measurements. After reaction completion, a few drops of HCl (1 M) were added to deactivate the catalyst, the mixture was concentrated, and the SCNPs (**N1** or **N2**) were isolated by precipitation in diethyl ether and further drying (**N1**: yield (%) = 79, $M_w$ (SEC/SLS) = 41 kDa, and $M_w/M_n$ = 1.05; **N2**: yield (%) = 75, $M_w$ (SEC/SLS) = 267.0 kDa, and $M_w/M_n$ = 1.25).

*2.4. SEC Analysis.* Size exclusion chromatography/static light scattering (SEC/SLS) measurements were performed at 30°C on an Agilent 1200 system equipped with PLgel 5 μm Guard and PLgel 5 μm MIXED-C columns, a differential refractive index (RI) detector (Optilab Rex, Wyatt), and a SLS detector

(Minidawn Treos, Wyatt). Data analysis was performed with ASTRA Software from Wyatt. THF was used as eluent at a flow rate of 1 mL/min. dn/dc values in THF as determined using the Optilab Rex detector online were found to be very similar for the precursors and SCNPs, so an average value of 0.083 was employed.

*2.5. IR Analysis.* Fourier transform infrared (IR) spectroscopy spectra were recorded at room temperature on a JASCO 3600 FTIR spectrometer.

*2.6. $^1$H NMR Analysis.* $^1$H nuclear magnetic resonance (NMR) spectra were recorded at room temperature on a Bruker spectrometer operating at 300 MHz.

*2.7. DLS Analysis.* Dynamic light scattering (DLS) on a Malvern Zetasizer Nano ZS apparatus was used to determine the hydrodynamic radius ($R_H$) of the samples at room temperature in THF solvent. The "size distribution by number" plot was employed in this work.

*2.8. EA Analysis.* Elemental analysis (EA) measurements were performed in a Euro EA3000 Elemental Analyzer (CHNS).

## 3. Results and Discussion

The synthetic procedure followed in this work towards SCNPs *via* intrachain amide formation is illustrated schematically in Figure 2.

As SCNP precursors, we targeted random copolymers of methyl methacrylate (MMA) and 2-acetoacetoxy ethyl methacrylate (AEMA) containing around 30 mol% of β-ketoester units and two different molecular weights (denoted by **P1** and **P2** in Table 1). It has been shown recently that by increasing the amount of functional groups above 30 mol% no significant increase in SCNP compaction is obtained [38, 39]. The precursors were synthesized by RAFT polymerization employing 2-cyanoprop-2-yl-dithiobenzoate (CPDB) as chain transfer agent and 2,2′-azobis(2-methylpropionitrile)

TABLE 1: Characteristics of precursors and SCNPs synthesized in this work by RAFT polymerization.

| Code | Yield (%) | $M_n$ (kDa)[a] | $M_w$ (kDa)[a] | $Đ = M_w/M_n$[a] | AEMA (mol%)[b] | Size (nm)[c] |
|------|-----------|----------------|----------------|------------------|----------------|--------------|
| **P1** | 46 | 39.1 | 40.9 | 1.05 | 30 | 9.5 |
| **P2** | 70 | 182.0 | 248.1 | 1.35 | 27 | 22.8 |
| **N1** | 79 | 39.0 | 41.0 | 1.05 | 30 | 6.4 |
| **N2** | 75 | 213.6 | 267.0 | 1.25 | 27 | 12.5 |

[a]As determined by SEC/SLS. [b]As determined by ^{1}H NMR spectroscopy. [c]As determined by DLS.

(AIBN) as free-radical initiator. RAFT is a very convenient polymerization technique for obtaining nanoparticle precursors with low molecular-weight polydispersity ($Đ = M_w/M_n$) and hence nanoparticles with uniform size [4]. The main characteristics of the random P(MMA-*co*-AEMA) copolymers investigated in this work are summarized in Table 1, as determined by size exclusion chromatography with absolute molar mass characterization (SEC/SLS), proton nuclear magnetic resonance (^{1}H NMR) spectroscopy, and dynamic light scattering (DLS). Well-defined copolymers displaying relatively low $Đ$ values were obtained. The lower yield of **P1** when compared to **P2** can be attributed to the higher amount of chain transfer agent employed in the former case, since polymerization time was identical for both precursors (18 h). A random placement of the $\beta$-ketoester moieties along the P(MMA-*co*-AEMA) chains is expected, due to the similar reactivity ratios of MMA and AEMA ($r_{MMA} = 0.90$ and $r_{AEMA} = 0.95$) during RAFT copolymerization, which are indicative of a statistical copolymerization process.

SCNPs were synthesized in THF at r.t., under anhydrous conditions, at high dilution (1 mg P(MMA-*co*-AEMA)/mL of THF), by addition of *ca.* 0.5 equivalents of the bifunctional isocyanate compound (HMDI) per equivalent of AEMA in the presence of DBN as catalyst (see Figure 2 and Table 1). Samples taken periodically from the reaction media were analyzed by SEC/SLS in THF. A progressive increase in SEC retention time and, hence, a concomitant reduction in P(MMA-*co*-AEMA) hydrodynamic size [40] were observed as a function of reaction time, pointing to the successful formation of SCNPs *via* intrachain amide formation (Figure 3). The same behavior was observed by employing **P2** instead of **P1** as SCNP precursor (data not shown). Direct evidence of amide formation between active methylene groups and isocyanate moieties was obtained by infrared (IR) spectroscopy. Figure 4 shows the appearance of four new IR vibration bands located at 1673, 1587, 1306, and 649 cm$^{-1}$ upon SCNP formation, which according to previous data reported in the literature [41] can be assigned to amide I, II, III, and V bands, respectively. In the IR spectrum of the SCNPs, also the presence of an –NH– vibration band located between 3100 and 3700 cm$^{-1}$ is observed (inset in Figure 4), which is very broad due to hydrogen bonding between amide groups. Similarly, the ^{1}H NMR spectrum of the SCNPs (Figure 5) shows characteristic signatures of amide formation [42]: (i) a peak located at 7.0 ppm coming from the protons of the new formed amide groups (–CO–NH–), (ii) a peak at 3.75 ppm from the methine protons (=CH–), (iii) a peak located at 3.5 ppm arising from
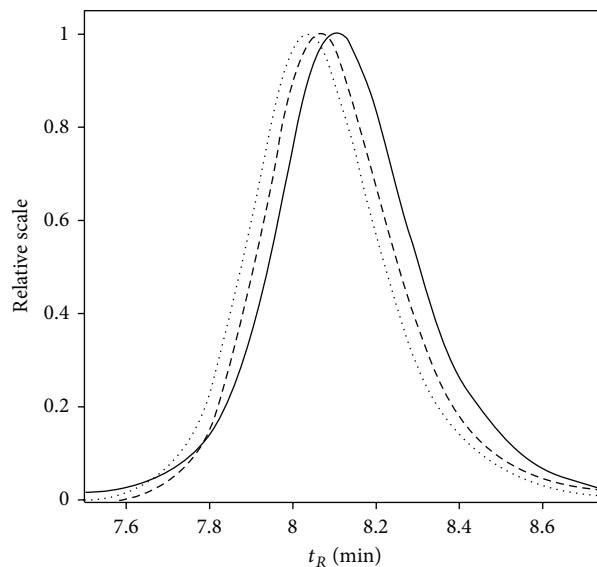


FIGURE 3: SEC/SLS traces showing the progressive reduction in hydrodynamic size of P(MMA-*co*-AEMA) copolymer **P1** upon intrachain cross-linking *via* amide formation. Reaction time: 0 h (dotted curve), 12 h (dashed curve), and 24 h (continuous curve).

methylene protons of the HMDI cross-linker next to the new formed amide group (–CO–NH–CH$_2$–), and (iv) a broad peak centered around 1.5 ppm assigned to internal methylene protons from the HMDI cross-linker (–CO–NH–CH$_2$–CH$_2$–). Further support of chain compaction upon SCNP formation was obtained from DLS measurements (see Table 1), which provided a measure of the hydrodynamic size of both the precursor and the SCNPs. As an example, a reduction in hydrodynamic size form 9.5 nm (precursor **P1**) to 6.4 nm (SCNP **N1**) was found upon SCNP formation, as illustrated in Figure 6. This significant reduction in size is in good agreement with the SEC/SLS results previously shown in Figure 3. Finally, elemental analysis (EA) was used to obtain a rough estimation of the amount of HMDI cross-linker incorporated into the SCNPs. A comparison of the theoretical composition by assuming a degree of amide formation of 100% and the corresponding experimental EA composition is shown in Table 2. From the ratio of the experimental to theoretical N content, a degree of intrachain cross-linking of *ca.* 97% was estimated.

TABLE 2: Comparison of the theoretical and experimental composition of P(MMA-*co*-AEMA) copolymers and SCNPs.

| Code | Theoretical | | | | Experimental[a] | | | |
|------|------|------|------|------|------|------|------|------|
| | C% | H% | O%[b] | N% | C% | H% | O%[b] | N% |
| **P1** | 58.12 | 7.30 | 34.58 | 0 | 58.26 | 7.39 | 34.35 | 0 |
| **N1** | 57.86 | 7.26 | 32.06 | 2.82[c] | 55.28 | 7.30 | 34.69 | 2.73 |
| **P2** | 58.15 | 7.38 | 34.47 | 0 | 57.92 | 7.41 | 34.67 | 0 |
| **N2** | 57.89 | 7.68 | 31.97 | 2.45[c] | 55.28 | 7.48 | 34.86 | 2.38 |

[a] As determined by EA. [b] Obtained as O% = 100 − (C% + H% + N%). [c] By assuming a degree of amide formation of 100%.
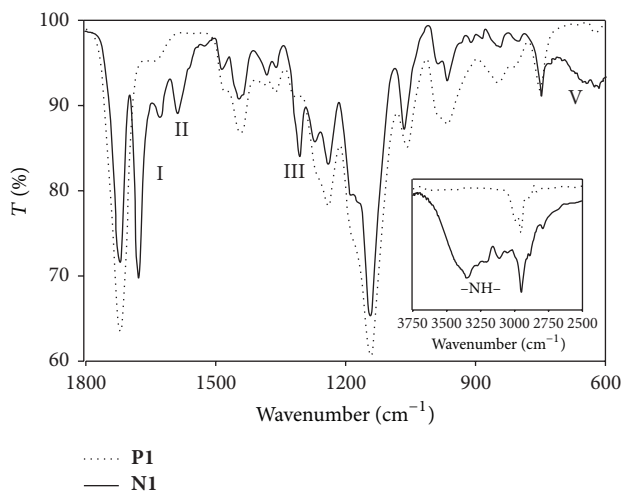


FIGURE 4: IR spectra of P(MMA-*co*-AEMA) copolymer **P1** (dotted trace) and SCNPs **N1** (continuous trace). New vibration bands observed in the IR spectrum of SCNPs **N1** upon amide formation are indicated (amide I, II, III, and V bands and –NH– band; see inset).
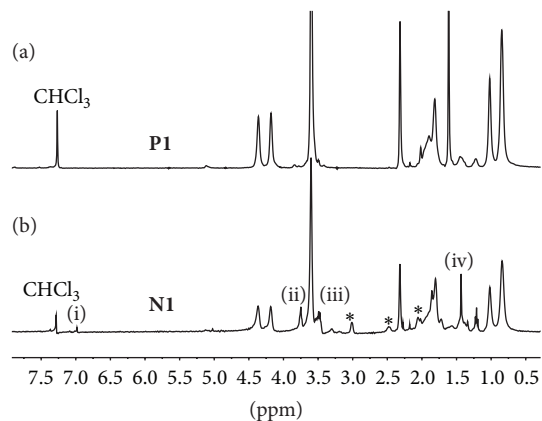


FIGURE 6: Hydrodynamic size distributions corresponding to P(MMA-*co*-AEMA) copolymer **P1** (dotted line) and SCNPs **N1** (continuous line), as determined by DLS measurements. For clarity reasons, only results for **P1** and **N1** are included. Data for **P2** and **N2** are provided in Table 1.



FIGURE 5: (a) $^1$H NMR spectra of P(MMA-*co*-AEMA) copolymer **P1** (for complete peak assignment, please refer to [37]). (b) $^1$H NMR spectra of SCNPs **N1**. New peaks observed in the $^1$H NMR spectrum of SCNPs **N1** upon amide formation are indicated (see text for assignment). Signals coming from traces of catalyst are indicated by asterisk.

copolymers of MMA and AEMA were synthesized by RAFT polymerization, showing low molecular-weight polydispersity and random placement of $\beta$-ketoester moieties along the P(MMA-*co*-AEMA) chains. Next, intramolecular collapse of these AEMA-containing copolymers as SCNP precursors was performed by the reaction at high dilution of AEMA $\beta$-ketoester moieties with hexamethylene diisocyanate cross-linkers in THF at r.t. Analysis of SEC/SLS, IR spectroscopy, $^1$H NMR spectroscopy, DLS, and EA results demonstrated the efficient synthesis of SCNPs *via* intrachain amide formation.

## Conflict of Interests

The authors declare that there is no conflict of interests regarding the publication of this paper.

## Acknowledgments

## 4. Conclusions

This work contributes to enlarging the toolbox of single-chain technology by demonstrating the efficient synthesis of SCNPs *via* intrachain amide formation. First, well-defined random
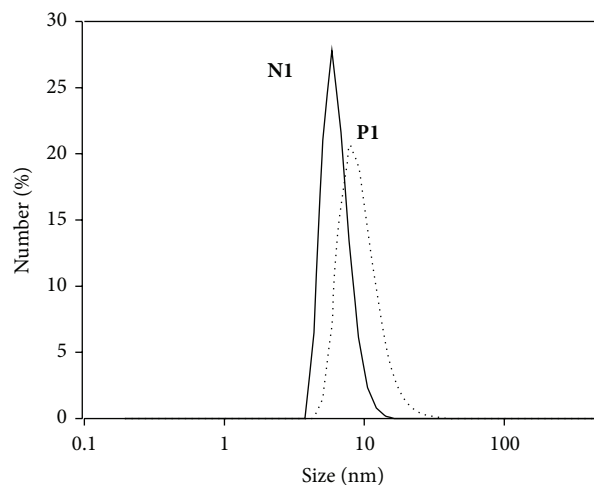
# References

[1] M. Ouchi, N. Badi, J.-F. Lutz, and M. Sawamoto, "Single-chain technology using discrete synthetic macromolecules," *Nature Chemistry*, vol. 3, no. 12, pp. 917–924, 2011.

[2] C. K. Lyon, A. Prasher, A. M. Hanlon et al., "A brief user's guide to single-chain nanoparticles," *Polymer Chemistry*, vol. 6, no. 2, pp. 181–197, 2015.

[3] A. Sanchez-Sanchez and J. A. Pomposo, "Single-chain polymer nanoparticles via non-covalent and dynamic covalent bonds," *Particle and Particle Systems Characterization*, vol. 31, no. 1, pp. 11–23, 2014.

[4] A. Sanchez-Sanchez, I. Pérez-Baena, and J. A. Pomposo, "Advances in click chemistry for single-chain nanoparticle construction," *Molecules*, vol. 18, no. 3, pp. 3339–3355, 2013.

[5] O. Altintas and C. Barner-Kowollik, "Single chain folding of synthetic polymers by covalent and non-covalent interactions: current status and future perspectives," *Macromolecular Rapid Communications*, vol. 33, no. 11, pp. 958–971, 2012.

[6] J. A. Pomposo, "Bioinspired single-chain polymer nanoparticles," *Polymer International*, vol. 63, no. 4, pp. 589–592, 2014.

[7] T. Terashima, T. Mes, T. F. A. de Greef et al., "Single-chain folding of polymers for catalytic systems in water," *Journal of the American Chemical Society*, vol. 133, no. 13, pp. 4742–4745, 2011.

[8] E. Huerta, P. J. M. Stals, E. W. Meijer, and A. R. A. Palmans, "Consequences of folding a water-soluble polymer around an organocatalyst," *Angewandte Chemie—International Edition*, vol. 52, no. 10, pp. 2906–2910, 2013.

[9] A. Sanchez-Sanchez, A. Arbe, J. Colmenero, and J. A. Pomposo, "Metallo-folded single-chain nanoparticles with catalytic selectivity," *ACS Macro Letters*, vol. 3, no. 5, pp. 439–443, 2014.

[10] A. Sanchez-Sanchez, S. Akbari, A. Etxeberria et al., "Michael nanocarriers mimicking transient-binding disordered proteins," *ACS Macro Letters*, vol. 2, no. 6, pp. 491–495, 2013.

[11] A. Sanchez-Sanchez, S. Akbari, A. J. Moreno et al., "Design and preparation of single-chain nanocarriers mimicking disordered proteins for combined delivery of dermal bioactive cargos," *Macromolecular Rapid Communications*, vol. 34, no. 21, pp. 1681–1686, 2013.

[12] D. Mecerreyes, V. Lee, C. J. Hawker et al., "A novel approach to functionalized nanoparticles: self-crosslinking of macromolecules in ultradilute solution," *Advanced Materials*, vol. 13, no. 3, pp. 204–208, 2001.

[13] J. Jiang and S. Thayumanavan, "Synthesis and characterization of amine-functionalized polystyrene nanoparticles," *Macromolecules*, vol. 38, no. 14, pp. 5886–5891, 2005.

[14] A. E. Cherian, F. C. Sun, S. S. Sheiko, and G. W. Coates, "Formation of nanoparticles by intramolecular cross-linking: following the reaction progress of single polymer chains by atomic force microscopy," *Journal of the American Chemical Society*, vol. 129, no. 37, pp. 11350–11351, 2007.

[15] E. Harth, B. van Horn, V. Y. Lee et al., "A facile approach to architecturally defined nanoparticles via intramolecular chain collapse," *Journal of the American Chemical Society*, vol. 124, no. 29, pp. 8653–8660, 2002.

[16] T. A. Croce, S. K. Hamilton, M. L. Chen, H. Muchalski, and E. Harth, "Alternative *o*-quinodimethane cross-linking precursors for intramolecular chain collapse nanoparticles," *Macromolecules*, vol. 40, no. 17, pp. 6028–6031, 2007.

[17] C. T. Adkins, H. Muchalski, and E. Harth, "Nanoparticles with individual site-isolated semiconducting polymers from intramolecular chain collapse processes," *Macromolecules*, vol. 42, no. 15, pp. 5786–5792, 2009.

[18] B. Zhu, J. Ma, Z. Li et al., "Formation of polymeric nanoparticles via Bergman cyclization mediated intramolecular chain collapse," *Journal of Materials Chemistry*, vol. 21, no. 8, pp. 2679–2683, 2011.

[19] B. Zhu, G. Qian, Y. Xiao, S. Deng, M. Wang, and A. Hu, "A convergence of photo-bergman cyclization and intramolecular chain collapse towards polymeric nanoparticles," *Journal of Polymer Science. Part A. Polymer Chemistry*, vol. 49, no. 24, pp. 5330–5338, 2011.

[20] X. Jiang, H. Pu, and P. Wang, "Polymer nanoparticles via intramolecular crosslinking of sulfonyl azide functionalized polymers," *Polymer*, vol. 52, no. 16, pp. 3597–3602, 2011.

[21] P. Wang, H. Pu, and M. Jin, "Single-chain nanoparticles with well-defined structure via intramolecular crosslinking of linear polymers with pendant benzoxazine groups," *Journal of Polymer Science, Part A: Polymer Chemistry*, vol. 49, no. 24, pp. 5133–5141, 2011.

[22] A. Sanchez-Sanchez, I. Asenjo-Sanz, L. Buruaga, and J. A. Pomposo, "Naked and self-clickable propargylic-decorated single-chain nanoparticle precursors via redox-initiated RAFT polymerization," *Macromolecular Rapid Communications*, vol. 33, no. 15, pp. 1262–1267, 2012.

[23] I. Perez-Baena, F. Barroso-Bujans, U. Gasser et al., "Endowing single-chain polymer nanoparticles with enzyme-mimetic activity," *ACS Macro Letters*, vol. 2, no. 9, pp. 775–779, 2013.

[24] E. H. H. Wong, S. J. Lam, E. Nam, and G. G. Qiao, "Biocompatible single-chain polymeric nanoparticles via organo-catalyzed ring-opening polymerization," *ACS Macro Letters*, vol. 3, no. 6, pp. 524–528, 2014.

[25] P. T. Dirlam, H. J. Kim, K. J. Arrington et al., "Single chain polymer nanoparticles via sequential ATRP and oxidative polymerization," *Polymer Chemistry*, vol. 4, no. 13, pp. 3765–3773, 2013.

[26] G. Li, F. Tao, L. Wang, Y. Li, and R. Bai, "A facile strategy for preparation of single-chain polymeric nanoparticles by intramolecular photo-crosslinking of azide polymers," *Polymer*, vol. 55, no. 16, pp. 3696–3702, 2014.

[27] P. Wang, H. Pu, J. Ge et al., "Fluorescence-labeled hydrophilic nanoparticles via single-chain folding," *Materials Letters*, vol. 132, pp. 102–105, 2014.

[28] A. R. de Luzuriaga, N. Ormategui, H. J. Grande, I. Odriozola, J. A. Pomposo, and I. Loinaz, "Intramolecular click cycloaddition: an efficient room-temperature route towards bioconjugable polymeric nanoparticles," *Macromolecular Rapid Communications*, vol. 29, no. 12-13, pp. 1156–1160, 2008.

[29] L. Oria, R. Aguado, J. A. Pomposo, and J. Colmenero, "A versatile 'click' chemistry precursor of functional polystyrene nanoparticles," *Advanced Materials*, vol. 22, no. 28, pp. 3038–3041, 2010.

[30] N. Ormategui, I. García, D. Padro, G. Cabañero, H. J. Grande, and I. Loinaz, "Synthesis of single chain thermoresponsive polymer nanoparticles," *Soft Matter*, vol. 8, no. 3, pp. 734–740, 2012.

[31] O. Altintas, J. Willenbacher, K. N. R. Wuest et al., "A mild and efficient approach to functional single-chain polymeric nanoparticles via photoinduced Diels-Alder ligation," *Macromolecules*, vol. 46, no. 20, pp. 8092–8101, 2013.

[32] W. Johannes, N. R. W. Kilian, J. O. Mueller, M. Kaupp, H. A. Wagenknecht, and C. Barner-Kowollik, "Photochemical

design of functional fluorescent single-chain nanoparticles," *ACS Macro Letters*, vol. 3, no. 6, pp. 574–579, 2014.

[33] J. É. F. Radu, L. Novak, J. F. Hartmann et al., "Structural and dynamical characterization of poly-gamma-glutamic acid-based cross-linked nanoparticles," *Colloid and Polymer Science*, vol. 286, no. 4, pp. 365–376, 2008.

[34] J. B. Beck, K. L. Killops, T. Kang et al., "Facile preparation of nanoparticles by intramolecular cross-linking of isocyanate functionalized copolymers," *Macromolecules*, vol. 42, no. 15, pp. 5629–5635, 2009.

[35] A. R. de Luzuriaga, I. Perez-Baena, S. Montes et al., "New route to polymeric nanoparticles by click chemistry using bifunctional cross-linkers," *Macromolecular Symposia*, vol. 296, no. 1, pp. 303–310, 2010.

[36] C. F. Hansell, A. Lu, J. P. Patterson, and R. K. O'Reilly, "Exploiting the tetrazine-norbornene reaction for single polymer chain collapse," *Nanoscale*, vol. 6, no. 8, pp. 4102–4107, 2014.

[37] A. Sanchez-Sanchez, D. A. Fulton, and J. A. Pomposo, "PH-responsive single-chain polymer nanoparticles utilising dynamic covalent enamine bonds," *Chemical Communications*, vol. 50, no. 15, pp. 1871–1874, 2014.

[38] I. Perez-Baena, A. J. Moreno, J. Colmenero, and J. A. Pomposo, "Single-chain nanoparticles vs. star, hyperbranched and dendrimeric polymers: effect of the nanoscopic architecture on the flow properties of diluted solutions," *Soft Matter*, vol. 10, no. 47, pp. 9454–9459, 2014.

[39] J. A. Pomposo, I. Perez-Baena, F. Lo Verso, A. J. Moreno, A. Arbe, and J. Colmenero, "How far are single-chain polymer nanoparticles in solution from the globular state?" *ACS Macro Letters*, vol. 3, no. 8, pp. 767–772, 2014.

[40] J. A. Pomposo, I. Perez-Baena, L. Buruaga, A. Alegría, A. J. Moreno, and J. Colmenero, "On the apparent SEC molecular weight and polydispersity reduction upon intramolecular collapse of polydisperse chains to unimolecular nanoparticles," *Macromolecules*, vol. 44, no. 21, pp. 8644–8649, 2011.

[41] M. Wöbkemeier and G. Hinrichsen, "Hydrogen bonding in aliphatic poly(amides)—dependence of infra-red spectra and density on chemical composition," *Polymer Bulletin*, vol. 21, no. 6, pp. 607–612, 1989.

[42] D. Esquivel, J. J. Bou, and S. Muñoz-Guerra, "Synthesis, characterization and degradability of polyamides derived from tartaric acid and diaminoethers," *Polymer*, vol. 44, no. 20, pp. 6169–6177, 2003.